CLUSTER VARIATION METHOD FOR FRUSTRATED MAGNETS
MÉTODO DE VARIACIÓN DE CLUSTERS EN MATERIALES MAGNÉTICOS FRUSTRADOS

E. Domínguez[†], A. Lage-Castellanos, C.E. Lopetegui and R. Mulet

Facultad de Física, Universidad de La Habana, 10400 La Habana, Cuba; edv2rd0@gmail.com[†]
† corresponding author

The model J_1-J_2 has provided a good theoretical benchmark for the study of frustrated magnets. This model is studied from the perspective of the Cluster Variation Method (CVM). In a first moment, Bethe approximation is considered. In this context it is possible to obtain a phase diagram where a stripes phase and a paramagnetic phase are observed, though separated by a non convergence zone. Secondly, plaquette approximation is considered and a complete phase diagram is obtained. In the latter it is observed an additional nematic phase with orientational but not positional order, which was not possible to observe using the Bethe approximation.

El modelo J_1-J_2 ha servido como base para el estudio teórico de materiales magnéticos frustrados. Este modelo es estudiado desde la perspectiva del Método de Variación de Clusters (CVM). En un primer momento se estudia utilizando la aproximación de Bethe. En este contexto se obtiene un diagrama de fases en el que es posible observar una fase de franjas y una fase paramagnética, separadas por una zona de no convergencia. Posteriormente se emplea la aproximación de plaquetas, lo cual permite obtener un diagrama de fases completo. En este último es posible observar la fase nemática, que no se observa al utilizar la aproximación de Bethe.

I. INTRODUCTION

Competing interactions are a common feature of many natural and artificial systems. Examples can be found in very different scenarios like solid state physics, mathematical optimization or quantum systems. In particular, ultra-thin magnetic films [2,3], spin glasses [4], high T_c superconductors [5–9], colloidal suspensions [10], and strongly correlated electron systems [11, 12], are some of the many examples where competing interactions are present. An interesting aspect when dealing with competing interactions is the arising of frustration, that is the inability of the system to satisfy all the interactions at the same time. High frustration gives place to very interesting and complex landscapes in the equilibrium (stripes, bubbles, clusters, spin liquid, disordered phases, etc). Also, to the occurrence of very complex phenomena such as slow relaxation to equilibrium and strong metastability [1].

One of the simplest models with competing interactions is the well known J_1-J_2 model. In a square lattice it is a simple extension of the Ising Model where, besides of the nearest neighbor (NN) ferromagnetic interaction characterized by the coupling factor J_1, one adds an antiferromagnetic interaction between next nearest neighbors (NNN) characterized by the parameter J_2.

The Hamiltonian describing the model is

$$H = -\sum_{\langle ij \rangle} J_1 s_i s_j - \sum_{\langle\langle ij \rangle\rangle} J_2 s_i s_j - \sum_i h_i s_i, \qquad (1)$$

where $\langle ij \rangle$ stands for the NN and $\langle\langle ij \rangle\rangle$ for the NNN.

This model has served as a paradigm for the study of frustrated magnets and a renewed attention has been put into it during the last decades [13–20]. The interest on the model is motivated by many factors.

In the very first place it is a simple model with a rich phase diagram [14, 20–22]. Depending on the adjustable parameter $k = |J_2/J_1|$ and the relative signs of the exchange interaction parameters, it offers the chance to describe Néel antiferromagnetic order (NAF), columnar antiferromagnetic order (CAF), or spin liquid and nematic phases.

It is precisely the evidence of the presence of the spin liquid phase [20, 21, 23], one of the reasons for the renaissance of the interest in the model. It is a fact that it provides a good opportunity to understand the spin liquid properties or even to obtain a realization of this type of order that conserves its properties near the absolute zero.

Besides, it is relevant for the understanding of high T_c superconductivity of cuprates and iron based superconductors such as LaFeAsO, that have shown superconductivity at temperatures up to 50 K [7–9, 24].

The recent experimental realization of "J_1-J_2 materials", such as $VOMoO_4$ [25], $Pb_2VO(PO_4)_2$ [21], Li_2VOSiO_4 and Li_2VOGeO_4 [26, 27], has open the gate for the necessity of a deep theoretical understanding of the model in order to compare with experimental results and make predictions.

Most of the theoretical work on the model has been devoted to the zero external field scenario [28–33], where a good understanding of the equilibrium properties has been reached already. In the case of the Ising J_1-J_2 in the zero field case for $k > 1/2$ a stripes phase of alternating up and down

spins is the ground state at low temperatures. The stripes phase is characterized by the presence of both orientational and positional order in the lattice.

On the other hand, nematic phases related to the stripe-like order are present in many quasi two dimensional systems like ultra-thin magnetic films and electronic liquids [34–38]. These nematic phases are characterized by the presence of orientational, but no positional order. In this sense there is an intermediate degree of symmetry between the disorder phase and the stripes (See Fig. 1 for an intuitive comprehension).
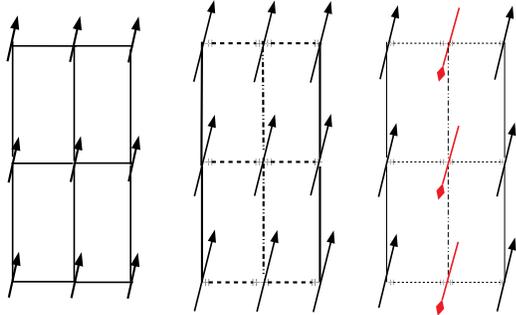

Figure 1. Schematic representation of order in the equilibrium state of the model. From left to right, paramagnetic (under homogeneous field), nematic and stripes order. Arrows stand for the mean local magnetization and lines for site to site correlations. **Left Paramagnetic**: All sites are equally tagged. There is no order at all, but a high symmetry. **Center Nematic**: Magnetizations are the same. However the correlation between horizontal neighbors is different from the correlation between vertical neighbors. There is orientational order characterized by non isotropic correlations. **Right Ferromagnetic**: Magnetization in the middle column point in an opposite direction to that of the rest of the sites. Correlations are just as in the nematic phase, so there is nor positional neither orientational order in the stripes phase.

A natural question arises: whether J_1-J_2 model would be able or not, to sustain such a nematic phase, as an intermediate phase in the breaking of the Z_4 symmetry of the disordered phase to the Z_2 symmetry of the stripes. The difficulty on the study of such anisotropic phases arises from the necessity of computing correlations in different directions.

In [22], Stariolo et al. answered the previous question by constructing an H-T phase diagram of the model. In this phase diagram it can be observed a region where nematic order arises. The phase diagram was built by using the well known Cluster Variational Method (CVM) approximation, which showed to be very appropriate for the study of anisotropic correlations. These authors point out that it is necessary to go beyond naive mean field (MF) and Bethe, in order to compute anisotropy in correlations. They asseverate that the minimal approximation suitable for detecting the stripes phase is the plaquette or Kikuchi approximation.

In the present paper we show that it is possible to observe the stripes phase in the context of the Bethe approximation, provided the regions and the symmetries of the problem are considered in a proper way. We will show the phase diagram of the problem, using both Bethe and the Kikuchi approximation, the latter resulting similar to the one reported in [22].

In order to differentiate the phases to which the model converges in equilibrium, two order parameters are used, one measuring the positional order and one measuring the orientational order. The orientational order parameter defined as

$$Q = \frac{1}{4}\left(l_{34} + l_{12} - l_{23} - l_{14}\right), \tag{2}$$

and the positional order parameter as

$$M = \frac{1}{2}\left(m_1 - m_4\right), \tag{3}$$

where $l_{ij} = \langle s_i s_j \rangle$ stands for the correlation between spins j and i, and m_i for the local magnetization at site i. The numeration follows Fig. 2
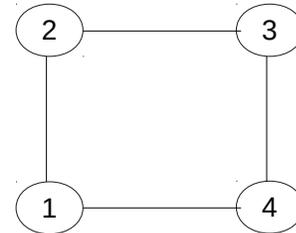

Figure 2. Sketch of the typical structure considered to compute the order parameters.

When the system is in the stripes phase both the order parameters are finite. The transition to disorder, where they are both zero, can occur in two ways. There can be a slow transition, characterized by a nematic intermediate order, or a discontinuous transition when both abruptly go to zero. Orientational order parameter plays the leading role when nematic order is present, and in fact, after leaving the stripes phase, there is no need to follow the behavior of the positional order.

As the largest correlations to be considered in order to compute these order parameters are links, it seems appropriate to consider at first instance the Bethe Approximation. This approximation considers links as largest regions in the Region Based Free Energy [39]. This will gives us the opportunity to consider different kind of interactions, which is not possible using Mean Field. In a second moment we consider the Kikuchy approximation which consider four site plaquettes as largest regions. This allows to take into account correlations among all four spins in the basic cell of the lattice, which improves the quality of the results.

II. BETHE APPROXIMATION

We study the equilibrium of the model using the CVM formalism [39]. The simplest approximation in this context is the Bethe-Peierls one, in which the largest regions considered in the variational free energy to minimize are links. It has been widely established that the constrained minimization of the Bethe free energy leads to a set of self-consistent equations in the Lagrange multipliers. Carefully treated, these equations result to map into the standard *Belief*

Propagation Algorithm (BP) equations [39]. In BP, Lagrange multipliers are understood as messages from links to sites. This algorithm is known to be exact in tree like graphs, and even when in structures with loops it does not give the exact results, it provides a simple and good insight into the equilibrium properties of a system.

The self-consistent equations for the messages have the form [39]

$$m_{j\to i}(s_i) = k_i \sum_{s_j} f(s_i, s_j) \prod_{k \in N(j)\backslash i} m_{k\to j}(s_j), \qquad (4)$$

where the message $m_{j\to i}(s_i)$ can be thought as the probability, as seen by the spin j that spin i has value s_i. The form of the functions $f(s_i, s_j)$ depends on whether spins i and j are NN or NNN. For NN it has the form

$$f(s_i, s_j) = \exp\left[\beta\left(J_1 s_i s_j + h_j s_j\right)\right], \qquad (5)$$

and for NNN

$$f(s_i, s_j) = \exp\left[\beta\left(J_2 s_i s_j + h_j s_j\right)\right]. \qquad (6)$$

It is usual to parametrize the messages as functions of cavity fields [40]

$$m_{j\to i}(s_i) = \exp\left[\beta u_{j\to i} s_i\right], \qquad (7)$$

where $u_{j\to i}$ has the form of a cavity field representing the influence of spin j over spin i.

It is useful to do so both because it improves the efficiency of the implementation and because it provides a very intuitive way to understand the messages.

The algorithm consists in solving the set of self-consistent equations by the fixed point iteration of the equations over the full lattice considering random initial values for the cavity fields. At every step new values are computed for the fields by taking the previous step ones, by means of the equation

$$u_{j\to i} = \frac{1}{\beta} \tanh^{-1}\left[\tanh\left(\beta J_{ij}\right)\tanh\left(\beta \sum_{k \in N(j)\backslash i} u_{k\to j}\right)\right], \qquad (8)$$

which is derived from equation 4.

All the important information of the system is finally obtained from the *beliefs* of each region. They represent the marginal distributions obtained for each region in the CVM framework. These beliefs approximate the exact Boltzmann marginals. If we moved in the CVM context to consider incrementally size regions the beliefs values should converge to that of the exact Boltzmann marginals.

Beliefs can be obtained in terms of the effective fields as

$$b_{ij}(s_i, s_j) = \frac{f(s_i, s_j)}{Z_{ij}} \exp\left(\sum_{k \in N(i)\backslash j} u_{k\to i} s_i + \sum_{k \in N(j)\backslash i} u_{k\to j} s_j\right) \qquad (9)$$

$$b_i(s_i) = \frac{1}{Z_i} \exp\left(h_i s_i + \sum_{k \in N(j)} u_{j\to i} s_i\right) \qquad (10)$$

At the time of the implementation it is possible to take advantage from the symmetry of the interactions. Supposing the whole lattice to be a repetition of a basic structure in the equilibrium, we can study the whole system by just considering some important links. In a way it is like removing the rest of the lattice without removing its influence. The important links are shown in Fig. 3. Not all the effective fields are represented there and the reason is that we make some considerations based on the symmetry of the interactions. In Fig. 3 a distinction is made between the sites of different columns. There are two reasons for this. The first one is that NN interactions are all defined by the same exchange parameter J_1 and the same for NNN interactions (J_2). Based on this, we are aware that the symmetry of the order phase should somehow be related to this fact. The form in which the order appears depends on the relation between J_1 and J_2. If $J_1 < J_2/2$, J_2 domains, otherwise J_1 does. The later is the case we are considering, so it is obvious to expect the symmetry of the stripes phase previously described. Considering this, we can reduce the amount of degrees of freedom (*d.o.f*) of the system to six effective fields, that are the ones in Fig. 3. So, the implementation we make is not the standard BP algorithm for lattices, but actually a fixed point calculation on the set of BP self-consistent equations for these six degrees of freedom.
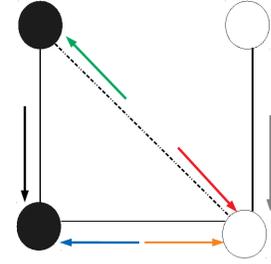

Figure 3. Representation of the relevant links in Bethe approximation.

In order to make it clear, for example, let's look at a horizontal link, it is the one between the sites represented black and white. The fields that enter into the update equations of the cavity fields between the two sites are represented in Fig. 4. The ones acting on the black spin enters into the update equation for the cavity field from the black site to the white one, and vice versa.
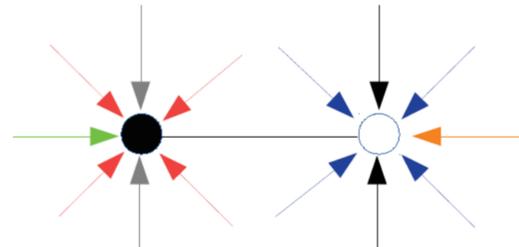

Figure 4. Fields that enter into the update equation for the effective fields in the link.

As a result of the Fixed Point study on this system it was possible to obtain an approximate phase diagram for the model (Fig. 5).

There are some important points to discuss about the phase diagram. First, it was possible to observe the stripes phase for low external magnetic fields and temperatures, which is in agreement with the results reported in [22]. On the other hand, the presence in this phase of anisotropic correlations seems to contradict their statement that the minimal approximation in which such a behavior could be observed is the Kikuchy one. The fact is that it is true only if you do not include in the Bethe region graphs the NNN links. So what we did was to include the diagonal links in the set of regions and consider the messages between NNN in the BP formulation.
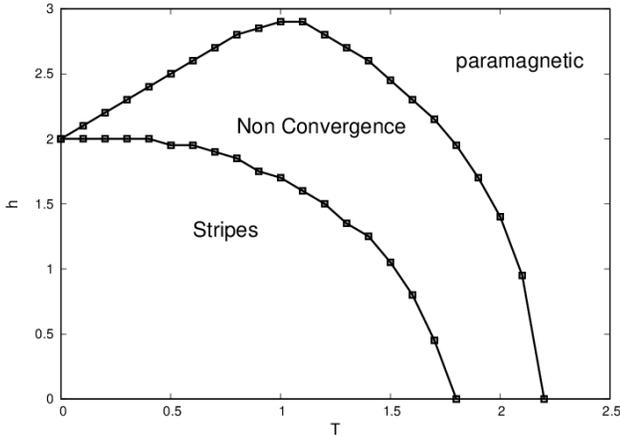

Figure 5. Phase diagram for J_1-J_2 model in the context of the Bethe Approximation.

For high temperatures and fields, it is predicted the existence of a paramagnetic phase, where nor orientational neither positional order are observed, and the average magnetization is only due to the presence of an external field.

On the other hand, a region of the diagram could not be described, as the algorithm did not converge. The reason why nematic phase could not be observed within this approximation is not completely clear to us, neither the reason of the non convergence. However, we will see below that it could be well connected with the appearence of the nematic phase.

Still, we want to emphasize that even when a complete characterization of the phase diagram is not possible at the Bethe level it proved again to be a useful tool in a fast exploration of the model.

III. PLAQUETTE APPROXIMATION

In order to obtain a more complete and accurate phase diagram for the model we go a step further in the CVM formalism and consider Kikuchi approximation. In this framework the largest regions to be taken into account in the construction of the variational free energy are the plaquettes of four sites. It is widely established that the constrained minimization of the Kikuchi free energy leads to a set of equations that are equivalent to those of the algorithm *Generalized Belief Propagation* [39]. In the *Parent to Child* formulation of the algorithm, messages go from parent

regions to children only, that is, from plaquettes to links, and from links to sites.

The objective is again to determine the marginal distributions for each region, which in this context are called *beliefs*. These beliefs are obtained from the equilibrium values of the messages by [40]

$$b_R\left(s_R\right) \alpha \prod_{a\in A_R} f_a\left(s_a\right) \left(\prod_{P\in\mathcal{P}(R)} m_{P\to R}\left(s_R\right) \right) \\ \prod_{D\in\mathcal{D}(R)} \prod_{P'\in\mathcal{P}(D)\setminus\varepsilon(R)} m_{P'\to D}\left(s_D\right),$$

(11)

where $f_a\left(s_a\right)$ has a similar meaning to that of $f\left(s_i,s_j\right)$,with the difference that for plaquettes, the expression includes all the pair interactions between the sites that conform it; $\mathcal{P}\left(R\right)$ stands for the parent regions of region R; $\mathcal{D}\left(R\right)$ for the regions descending from R; and $\varepsilon\left(R\right)$ represents the set formed by R and its descendants.

It is important to notice that at the time of constructing the region based free energy, links between NNN sites are not included as they have counting number zero, which is logical if we realize that they are not part of any intersection of larger regions.

Again it is appropriate to parametrize the messages in terms of cavity fields [40]. The messages from links to spin have the form stated in (7). On the other side, the parametrization of plaquette to link messages is more subtle. This is

$$M_{\mathcal{P}\to\mathcal{L}}\left(s_i,s_j\right) = \exp\left[\beta\left(U_{\mathcal{P}\to\mathcal{L}}\right)s_i s_j + u_{\mathcal{P}\to i}s_i + u_{\mathcal{P}\to j}s_j\right],$$

(12)

where $U_{\mathcal{P}\to\mathcal{L}}$ has the form of an effective interaction term like J_{ij} and the other terms have a similar meaning to that of the cavity fields that parametrize link to spin messages.

Some symmetry considerations were made before the implementation. In the first place, as it can be predicted from the results in the Bethe context, and as it is known from [22], the higher possible degree of order for the model is that of the stripes phase. Based on that, it is possible to impose some constrains over the values of the messages. This idea is shown in Fig. 6 where we show that some messages are taken to be the same, in the way it should be in the stripes phase. In this figure messages from the plaquette P to its children are not represented, but they are to be considered equivalent to the ones coming from neighbor plaquettes. Notice that doing this represents a great simplification of the computational requirements as we reduce the problem to a set of eleven selfconsistent equations.

We consider a characteristic plaquette to reproduce the behavior of the entire lattice, considering the effect of the rest of the system through the messages or in our case the cavity fields from nearby regions (Fig. 6). In this way our computation translates into a *Fixed Point* calculation on the set of GBP self-consistent equations for the fields remaining
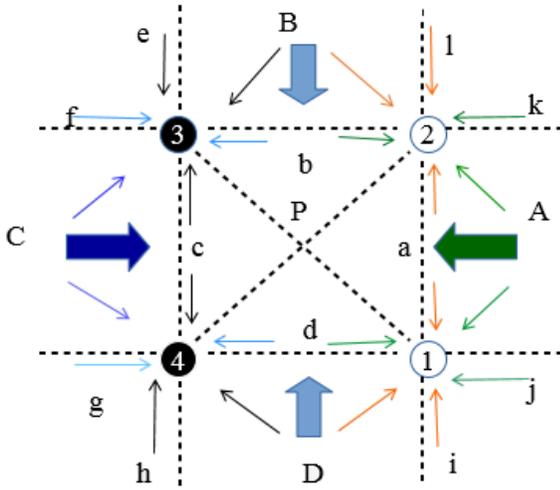
in the structure.

Figure 6. Structure over which the algorithm is run and the constrains over the messages.

Following the ideas outlined in [40], we can remove the *gauge* invariance in the cavity field equations. The standard parent-to-child implementation of the GBP method introduces more parameters than actually needed [40, 41] to characterize the local beliefs distributions. The redundant parameters do not alter the fixed point solution, but could affect the convergence of the fixed point algorithm. So, based on the recommendation in the previous reference, we set two of the field variables to be zero. In Fig. 7 we omit the fields that we force to be zero.
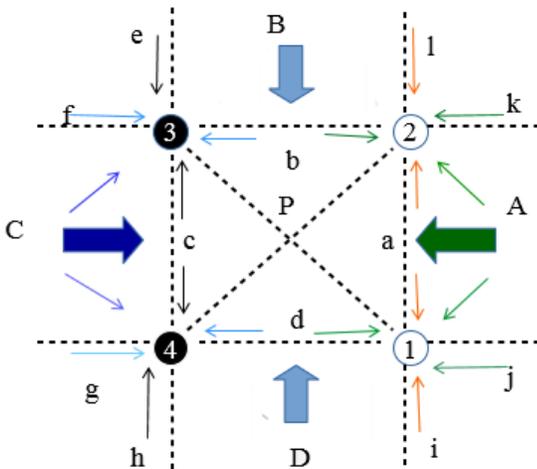

Figure 7. Structure over which the *Fixed Point* calculation is done, and constrains over the fields. The ones forced to be zero are omitted in this sketch.

On the other hand, there is a set of fields which enter into the update equation of each other partly linearly, which usually slows down the convergence. It can be avoided by solving the linear system they form, in function of the non linear parts of the update equations. Doing this drastically improves the convergence of the algorithm.

In this context it was obtained a complete phase diagram (Fig. 8), similar to that in [22].
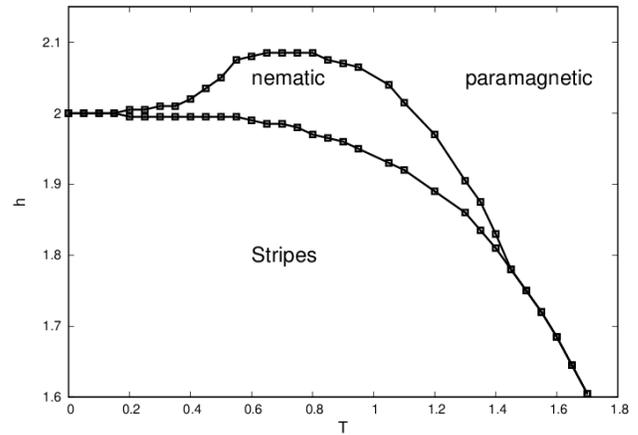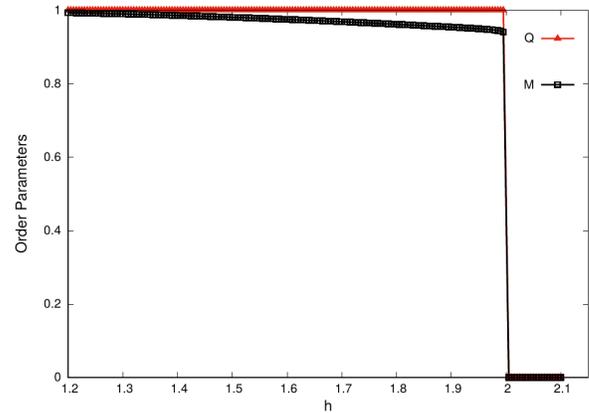

Figure 8. Phase Diagram using GBP.

Figure 9. Order parameters as a function of h for $T = 0.05$. A discontinuous transition is observed for both of the parameters. So, the transition from stripes to paramagnetic phase is direct.
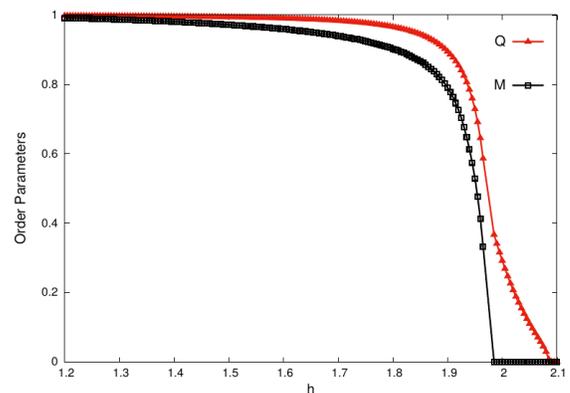

Figure 10. Order parameters as a function of h for $T = 0.8$. It can be observed a first transition in which positional order goes to zero while there is still orientational order. This is the signature of the nematic phase. A second transition occurs in which orientational order goes continuously to zero, so that paramagnetic phase is reached. At this temperature, transition from order phase (that is, from stripes), to disorder, occurs by passing through an intermediate nematic type order, rather than directly as at $T = 0.05$.

It is important to notice that at very low temperatures the transition from the stripes ordered phase to the paramagnetic

one seems to occur directly without passing through the nematic order, which is the main difference with the results published in [22]. In order to make it clear we show the behavior of the order parameters as a function of the external field for $T = 0.05$ (Fig. 9).

On the other hand we can look at the behavior of these parameters for $T = 0.8$, where the nematic phase is clearly observed (Fig. 10).

IV. CONCLUSIONS

In this work we studied the J_1-J_2 using the Cluster Variational Method. By considering the proper symmetries of the model, it was possible for the first time in the literature, to describe the presence of stripes in the Bethe approximation. Unfortunately the Bethe approximation does not converge for all the parameters of the model.

We improved over Bethe by studying also the model in the plaquette or Kikuchi approximation. In this case, the full phase diagram is accessible without convergence issues, and in addition to the stripes and the paramagnetic phases, we show the existence of a nematic phase. Our results are mostly consistent to the ones in [22]. However the phase diagram in [22] was computed through a numerical minimization of the Kikuchi free energy, while our results come from the exact solution of the fixed point equations obtained after the analytical minimization of an equivalent free energy. Both methods have advantages and disadvantages of their own, but certainly fixed point equations usually provides faster convergence (if they converge).

We are able to show a finer description of the low temperature extreme of the transition curves. In [22] it is suggested that the nematic phase is stable for any $T > 0$. Our results, on the contrary, point to the presence of a minimum $T_c(h_c) \simeq 0.2$. Below this temperature the nematic phase does not exist and the transition occurs directly between the paramagnetic to the stripe phase.

REFERENCES

[1] D. Wales, Cambridge University Press, Cambridge, 2003.

[2] K. De'Bell, A.B. MacIsaac and J.P. Whitehead, Rev. Mod. Phys. **72**, 225, (2000).

[3] A. Vaterlaus, C. Stamm, U. Maier, M.G. Pini, P. Politi and D. Pescia, Phys. Rev. Lett. **84**, 2247, (2000).

[4] K.H. Fischer and J.A. Hertz, Cambridge University Press, Cambridge, 1991.

[5] E. Fradkin, S.A. Kivelson, M.J. Lawler, J.P. Eisenstein and A.P. Mackenzie, Annu. Rev. Condens. Matter Phys. **1**, 153, (2010).

[6] E. Berg, E. Fradkin, S.A. Kivelson and J.M. Tranquada, New Journal of Physics **11**, 115004, (2009).

[7] Q. Si and E. Abrahams, Phys. Rev. Lett. **101**, 076401, (2008).

[8] C. Fang, H. Yao, W.F. Tsai, J.P. Hu and S.A. Kivelson, Phys. Rev. B **77**, 224509, (2008).

[9] T. Yildirim, Phys. Rev. Lett. **101**, 057010, (2008).

[10] D. Coslovich, M. Bernabei and A.J. Moreno, J. Chem. Phys. **137**, 184904, (2012).

[11] V.J. Emery, S.A. Kivelson and E. Fradkin, Nature **393**, 550, (1998).

[12] E. Fradkin and S.A. Kivelson, Phys. Rev. B **59**, 8065, (1999).

[13] T. Aoki, J. Phys. Soc. Jpn. **73**, 599, (2004).

[14] E. Dagotto and A. Moreo, Phys. Rev. Lett. **63**, 2148, (1989).

[15] M. Mambrini, A. Láuchli, D. Poilblanc and F. Mila, Phys. Rev. B **74**, 144422, (2006).

[16] X.G. Wen, Phys. Rev. B **44**, 2664, (1991).

[17] R. Darradi, O. Derzhko, R. Zinke, J. Schulenburg, S.E. Krúger and J. Richter, Phys. Rev. B **78**, 214415, (2008).

[18] M.E. Zhitomirsky and K. Ueda, Phys. Rev. B **54**, 9007, (1996).

[19] N. Read and S. Sachdev, Phys. Rev. Lett. **62**, 1694, (1989).

[20] H.C. Jiang, H. Yao and L. Balents, Phys. Rev. B **86**, 024424, (2012).

[21] N. Shannon, B. Schmidt, K. Penc and P. Thalmeier, Eur. Phys. J. B **38**(4), 599, (2004).

[22] A.I. Guerrero, D.A. Stariolo and N.G. Almarza, Phys. Rev. E **91**, 052123, (2015).

[23] P.W. Anderson, Materials Research Bulletin **8**(2), 153, (1973).

[24] K. Seo, B.A. Bernevig and J. Hu, Phys. Rev. Lett. **101**, 206404, (2008).

[25] P. Carretta, N. Papinutto, C.B. Azzoni, M.C. Mozzati, E. Pavarini, S. Gonthier and P. Millet, Phys. Rev. B **66**, 094420, (2002).

[26] H. Rosner, R.R.P. Singh, W.H. Zheng, J. Oitmaa and W.E. Pickett, Phys. Rev. B **67**, 014416, (2003).

[27] R. Melzi, S. Aldrovandi, F. Tedoldi, P. Carretta, P. Millet and F. Mila, Phys. Rev. B **64**, 024409, (2001).

[28] S. Jin, A. Sen and A.W. Sandvik, Phys. Rev. Lett. **108**, 045702, (2012).

[29] A. Kalz, A. Honecker, S. Fuchs and T. Pruschke, J. Phys.: Conf. Ser. **145**(1), 012051, (2009).

[30] A. Kalz, A. Honecker and M. Moliner, Phys. Rev. B **84**, 174407, (2011).

[31] J.L. Morán-López, F. Aguilera-Granja and J.M. Sanchez, Phys. Rev. B **48**, 3519, (1993).

[32] J.L. Moran-Lopez, F. Aguilera-Granja and J.M. Sanchez, J. Phys.: Condens. Matter **6**(45), 9759, (1994).

[33] R.A. dos Anjos, J.R. Viana and J.R. de Sousa, Phys. Lett. A **372**(8), 1180, (2008).

[34] D.G. Barci, A. Mendoza-Coto and D.A. Stariolo, Phys. Rev. E **88**, 062140, (2013).

[35] S.A. Cannas, M.F. Michelon, D.A. Stariolo and F.A. Tamarit, Phys. Rev. B **73**, 184425, (2006).

[36] N.G. Almarza, J. Pekalski and A. Ciach, J. Chem. Phys. **140**(16), 164708, (2014).

[37] L. Nicolao and D.A. Stariolo, Phys. Rev. B **76**, 054453, (2007).

[38] Ar. Abanov, V. Kalatsky, V.L. Pokrovsky and W.M. Saslow, Phys. Rev. B **51**, 1023, (1995).

[39] W.T. Freeman, J.S. Yedidia and Y. Weiss, TR2004-040, (2004).

[40] E. Domínguez, A. Lage-Castellanos, R. Mulet, F. Ricci-Tersenghi and T. Rizzo, Journal of Statistical Mechanics: Theory and Experiment **2011**(12), 12007, (2011).

[41] E. Domínguez, A. Lage-Castellanos, R. Mulet and F. Ricci-Tersenghi, Phys Rev E **95**, 043308, (2017).